Modeling Earth Systems and Environment (2025) 11:422
https://doi.org/10.1007/s40808-025-02623-5

ORIGINAL ARTICLE

Soil erosion projection based on the CMIP6 multi-model ensemble, case study of Wadi El-Ham watershed, northern Algeria

kamel Deia[1] · Mahmoud Hasbaia[1] · Zekai Şen[2] · Omar Djoukbala[1]

Received: 29 May 2025 / Accepted: 4 September 2025

Abstract
This study uses the Revised Universal Soil Loss Equation (RUSLE) to estimate both historical (1990–2011) and future (2026–2050) soil-loss rates in the Wadi El-Ham watershed in northern Algeria under three CMIP6 climate scenarios (SSP1-2.6, SSP2-4.5, SSP5-8.5). Monthly precipitation (1975–2011) measured from eight meteorological stations and CMIP6 multi-model ensemble data from the IPCC AR6 Interactive Atlas were used to derive rainfall erosivity, with the delta method applied to correct bias for improve the quality of the results. Spatial inputs for soil erodibility, topography and land cover were derived from FAO soil maps, a 30 m DEM, and Landsat imagery ; respectively. The obtained results show a historical specific soil loss of 5.18 t ha^{-1} yr^{-1}, predominantly concentrated on steep northern slopes, while more than half of the watershed experienced low erosion rates. The specific soil loss projected for the period 2026–2050 is expected to decrease by 24–29% compared to the historical period, with little change across scenarios (3.72–3.92 t ha/yr) and a slight contraction is expected in the most vulnerable areas, with continued vulnerability in the northern plateaus. The results of this study can guide erosion mitigation measures by identifying the most vulnerable areas. Furthermore, by highlight the key sources of uncertainty and challenges in modeling future erosion, they provide researchers with a basis for testing innovative approaches to address these limitations.

Keywords Soil erosion · Wadi El-Ham watershed · Algeria · RUSLE · Bias correction · CMIP6

Introduction

Soil erosion is one of the most dangerous natural events that directly impacts agricultural lands, crops, and water resources, increasing the risk of landslides and damage to facilities and property (Sartori et al. 2019). Soil erosion occurs primarily through water, wind, tillage, and harvesting processes, with water erosion (sheet, gully, and stream) being the most common (Borrelli et al. 2021).

Globally, water erosion accounts for approximately 55% of eroded land, making it the most common type of soil degradation, with an annual erosion rate estimated at 10.2 tons/ha/year (Li and Fang 2016). More than 24% of agricultural land worldwide is at risk of severe erosion, equivalent to a financial loss of hundreds of billions of dollars (Sartori et al. 2019). At the national level, soil erosion affects 7 million hectares of agricultural land in Algeria (Djoukbala et al. 2022), directly impacting their productivity. This also exacerbates another phenomenon: silting of dams, where the amount of sediment is increasing by 45 million tons annually in Algeria (Remini and Hallouche 2007). This poses a real threat to scarce water resources, especially with the increase in demand and the worsening drought.

Climate change is one of the main factors exacerbating soil erosion by altering rainfall and temperature patterns, plant biomass productivity, soil properties, and land management practices (Li and Fang 2016). The frequency and intensity of extreme events are expected to increase in the

✉ kamel Deia
kamel.deia@univ-msila.dz

Mahmoud Hasbaia
mahmoud.hasbaia@univ-msila.dz

Zekai Şen
zsen@medipol.edu.tr

Omar Djoukbala
omar.djoukbala@univ-msila.dz

[1] CEHSD Laboratory, University of M'sila, 28000 M'Sila, Algeria

[2] Faculty of Engineering, Istanbul Medipol University, Istanbul, Turkey

Published online: 18 September 2025

coming decades, which directly leads to increased runoff and soil particle detachment due to raindrops, thus increasing the risk of erosion (Weng et al. 2023). Furthermore, soil is an important carbon store; this is because soil erosion can contribute to climate change by redistributing soil organic carbon and affecting sequestration and emission pathways, thus impacting the global carbon cycle (Borrelli et al. 2017; García-Ruiz et al. 2017).

Researchers worldwide have used a variety of modeling approaches to assess soil erosion, including empirical (e.g., USLE, RUSLE), physical models (e.g., WEPP, LISEM), process-based models (e.g., SWAT, EUROSEM), and statistical models (e.g., FUZZY, CF) (Pandey et al. 2021). Empirical models have a simple structure and require limited input data, but they cannot simulate detailed hydrological and sediment transport processes. In contrast, Physical and process-based models have a more complex structure than empirical models and can simulate sediment transport and deposition, as well as the effects of land use change, but they require extensive datasets and computational resources (Raza et al. 2021; Pandey et al. 2021). However, throughout the history of modelling, the Revised Universal Soil Loss Equation (RUSLE) model is considered the most widely used worldwide due to its high degree of flexibility, abundant data and low cost (Alewell et al. 2019). It is a straightforward empirical model that expresses erosion rates in long-term averages based on topographical and environmental criteria, in addition to slowly changing land cover management over time (Sartori et al. 2019).

Understanding future climate scenarios is crucial to making the right decisions to adapt to their potential impacts. Climate models simulate the interactions within the Earth's climate system and are the best way to predict changes in precipitation, temperatures, and other climate variables. CMIP6 (Coupled Model Intercomparison Project phase 6) is considered the latest generation of such models, which is considered an improvement to CMIP5 by including new emission and detailed land use scenarios, the inclusion of additional components of the earth system, and other improvements (Almazroui et al. 2020; Sahabi-Abed et al. 2023). These models are subject to continuous development and allow for more accurate and comprehensive climate predictions. In this context, several studies in Algeria have used CMIP6 climate models to assess the impacts of climate change, focusing primarily on temperature and precipitation projections (Sahabi-Abed et al. 2023; Chetioui and Bouregaa 2024; Belazreg et al. 2023; Hamitouche et al. 2024). However, very few studies have evaluated future soil erosion in relation to these projections, highlighting an important research gap that this study seeks to address. In contrast, several studies in other parts of North Africa, such as Tunisia and Morocco, have addressed this issue and reported mixed results, with some predicting increased soil erosion in the future and others indicating a decrease (Bammou et al. 2024; Jarray et al. 2025; Lamane et al. 2025).

Uncertainty is considered as one of the major challenges facing climate modeling, including several identified sources of uncertainty, such as to uncertainty from internal climate fluctuations, climate models and emission scenarios (Sauchyn et al., 2022). However, the amount of uncertainty is not the same in all cases, since it varies depending on the variable, the size and location of the target area, and the time period (Sauchyn et al., 2022). For example, precipitation estimates, and related variables are considered less precise compared to temperature estimates. To reduce uncertainty, it is important for researchers to seek solutions with multi-model ensembles rather than individual models under various emission scenarios, as MMEs perform better and increase the reliability of the estimates (Mohobane et al. 2014; Sauchyn et al. 2022).

Assessing the impacts of climate change at regional scales—particularly for soil erosion—requires high-resolution data, which are not directly available from coarse-resolution global climate models. To overcome this problem, researchers resort to downscaling and bias correction techniques, through which the quality, spatial and temporal accuracy of these data can be improved (Almazroui et al. 2020a). There are two main approaches in downscaling methods: dynamic and statistical downscaling, where the first one is based on high-resolution regional climate models RCMs based on global model GCMs data, while the second approach is based on establishing a statistical relationship between local climate variables and large-scale variables (Schmidli et al. 2006), among which there are various techniques such as regression models, weather generators, weather typing schemes.

This study aims to assess historical (1990–2011) and future (2026–2050) soil erosion in the Wadi El-Ham watershed under different climate scenarios using the RUSLE equation and the CMIP6 multi-model ensemble. To obtain more accurate results, we applied the delta method to correct for bias in rainfall data. This study contributes to identifying the direct impact of climate change on soil erosion in the study area, a typical semi-arid environment, and highlighted Understanding future climate scenarios is crucial to making the right decisions to adapt to their potential impacts.

Materials and methods

Study area

The study focuses on the Wadi El-Ham watershed, a significant hydrological unit in northern Algeria. Geographically,

the watershed is situated between 35°15′ and 36°15′ north latitude and between 3° and 4°15′ east longitude and is approximately 150 km from the Mediterranean Sea. (Fig. 1) It covers an area of approximately 5594 km², with a perimeter of about 492 km. The topography shows considerable variability, with elevations ranging from around 444 m to as high as 1800 m. This range in elevation contributes to diverse climatic and hydrological conditions between the north and south.

Data

This study uses multiple datasets to assess actual and future soil erosion in the Wadi Al Ham watershed. Although the study area and surrounding watersheds contain many stations, some have missing records. To minimize errors, the period 1975–2011 was selected, using monthly observed data from only eight reliable stations (Table 1) provided by the Agence Nationale des Ressources Hydrauliques (ANRH) https://www.pseau.org/outils/organismes/organisme_detail.php?org_organisme_id=13855&l=fr.

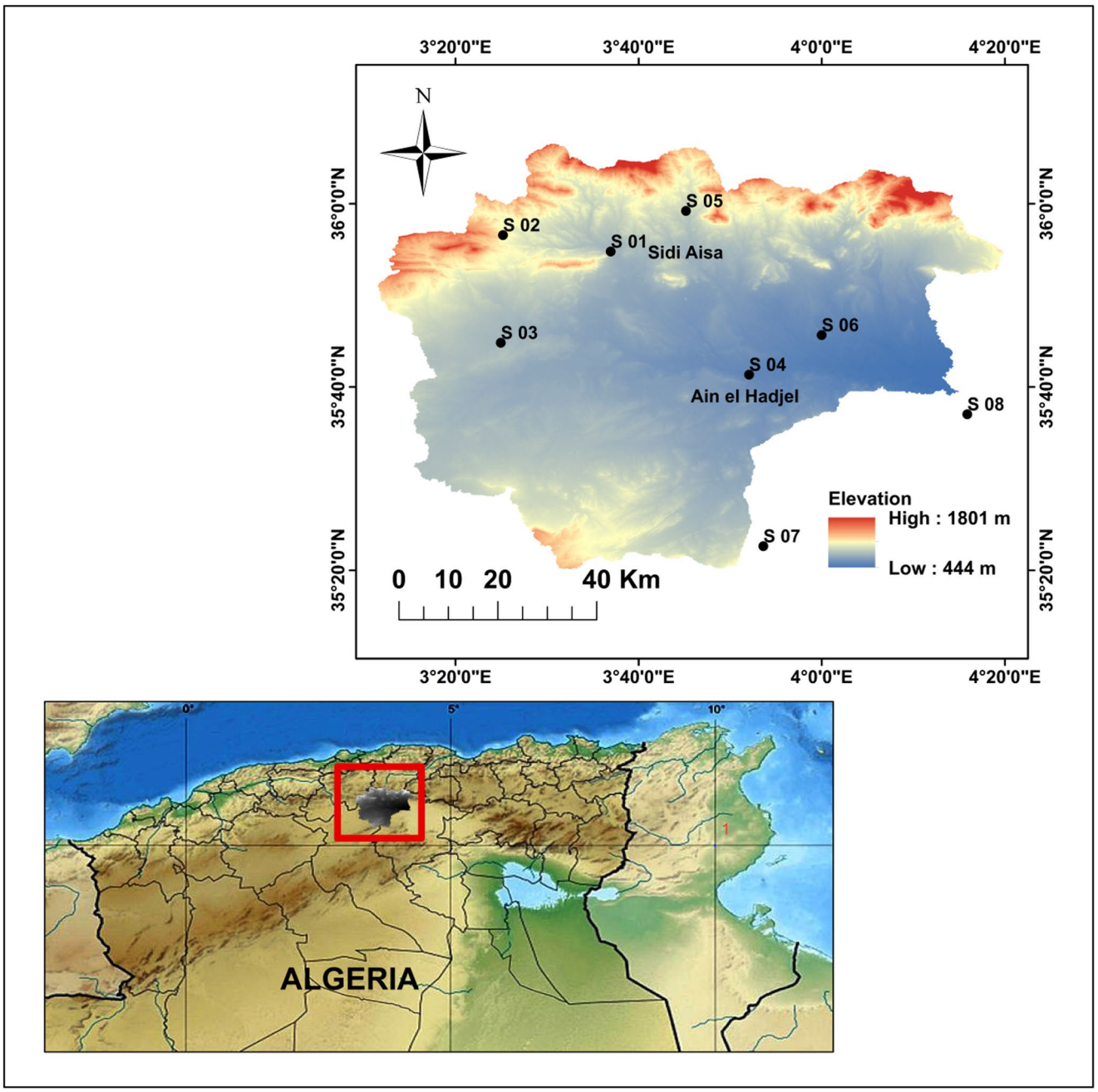

Fig. 1 Map of Wadi El-Ham watershed

Table 1 Rainfall gauging stations informations

Station	Name	Longitude	Latitude
S01	AIN NESSISSA	3.616°E	35.913°N
S02	CHELLALET EL ADAOURA	3.420°E	35.943°N
S03	DRAA EL HADJAR	3.416°E	35.747°N
S04	AIN EL HADJEL	3.860°E	35.680°N
S05	DIRAH CENTRE	3.753°E	35.987°N
S06	MEIDA	4.000°E	35.761°N
S07	SIDI AMEUR	3.894°E	35.377°N
S08	ROCADE SUD	4.265°E	35.617°N

In cases where data were missing for a given month, the gap was filled using the long-term average for that same month from the other available years.

While historical (1975–2011) simulations and future (2026–2050) monthly precipitation projections were obtained from the CMIP6 multi-model ensemble (1° resolution) via the Copernicus Climate Data Store (Atlas portal) https://atlas.climate.copernicus.eu/ under SSP1-2.6, SSP2-4.5, and SSP5-8.5 scenarios, the number of available models varies according to the emission scenario (SSP1-2.6 (31), SSP2-4.5 (32), SSP5-8.5 (33)). Figure 2 shows the available models corresponding to the historical data and each emission scenario. A bias correction (delta method) was applied using 1975–1999 monthly precipitation data for calibration and 2000–2011 for validation to improve model accuracy. Soil data from the FAO Soil Map were used to derive erodibility factor (K-factor), while Landsat 8 images are used to estimate the land cover factor (C-factor). A 30 m DEM was utilized to calculate the LS-factor, representing topographic influence on erosion. These datasets enable a comprehensive evaluation of soil erosion trends and future risks under variables climate conditions.

Delta method for bias correction

This method is utilized for bias correction of precipitation data through a simple and straightforward statistical technique widely applied in climate science and hydrology. It serves as a tool to estimate local or regional climate variables such as precipitation or temperature, by downscaling the output of global climate models (GCMs) or regional climate models (RCMs). This method works on a basic principle based on the concept of change or "delta" between observed historical and modeled climate data by quantifying the differences between observed and modeled data over a reference period. This method is computationally simple, requires less data, and preserves typical trends in climate projections. In many cases, the performance of this method in bias correction is better than some other more complex methods such as quantile mapping (QM) techniques (Beyer et al. 2020; Mendez et al. 2020) However, the performance of each method may vary according to each individual case (Beyer et al. 2020). In this study, we applied the multiplicative delta method for precipitation according to the following expressions.

$$P_{BC-Fut} = P_{GCM-SSP} \times \overline{P}_{obs}/\overline{P}_{GCMhist} \quad (1)$$

$$P_{BC-Eval} = P_{GCMhist} \times \overline{P}_{obs}/\overline{P}_{GCMhist} \quad (2)$$

$\boldsymbol{P_{BC-Fut}}$: represent bias-corrected precipitation data for the future period.

$\boldsymbol{P_{GCM-SSP}}$the data extracted from Global Climate Models (GCMs) across different Shared Socioeconomic Pathways (SSPs).

$\boldsymbol{\overline{P}_{obs}}$: observed average precipitation during a specific period.

$\boldsymbol{\overline{P}_{GCMhist}}$: the GCMs mean simulation data for historical precipitation records.

$\boldsymbol{P_{BC-Eval}}$: represent bias-corrected precipitation data, designed for the evaluation period.

$\boldsymbol{P_{GCMhist}}$the GCMs simulation data for historical precipitation records.

The performance of the bias correction was assessed using three statistical indicators:

- Percent Bias (PBIAS) (Eq. 3), indicates the average tendency of the simulated values to overestimate or underestimate the observations.
- Root Mean Square Error (RMSE) (Eq. 4), measures the magnitude of the differences between simulated and observed values, expressed in millimeters.
- Normalized RMSE (nRMSE) (Eq. 5), which is the RMSE expressed as a percentage of the observed mean rainfall, providing a scale-independent measure.

$$\boldsymbol{PBIAS}\,(\%) = \frac{(\overline{P}_{GCMhist} - \overline{P}_{obs})}{\overline{P}_{obs}} \times 100 \quad (3)$$

$$\boldsymbol{RMSE} = \sqrt{\frac{\sum_{i=1}^{n}(\boldsymbol{P_{GCMhist,\,i}} - \boldsymbol{P_{obs,\,i}})^2}{\boldsymbol{n}}} \quad (4)$$

$$\boldsymbol{nRMSE}\,(\%) = \frac{\boldsymbol{RMSE}}{\overline{P}_{obs}} \times 100 \quad (5)$$

Where $P_{GCMhist,\,i}$ and $P_{obs,\,i}$ are the modeled and observed precipitation values for month .

$\overline{P}_{obs}$ is the mean observed precipitation, and $\boldsymbol{n}$ is the number of observations.

An overiew of the methodological farmework adopted in this study is presented in Fig. 3.

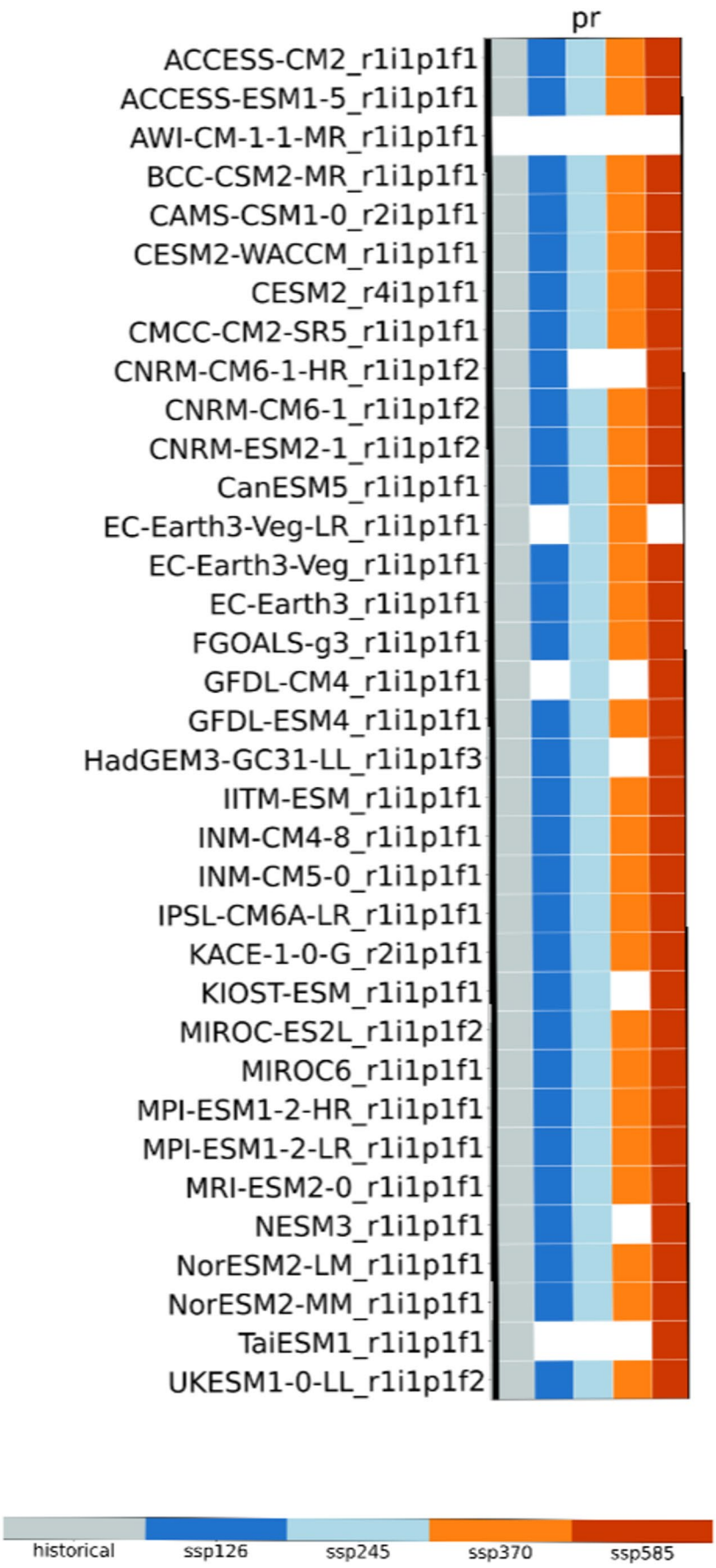

Fig. 2 List of CMIP6 GCMs and their scenario availability for precipitation

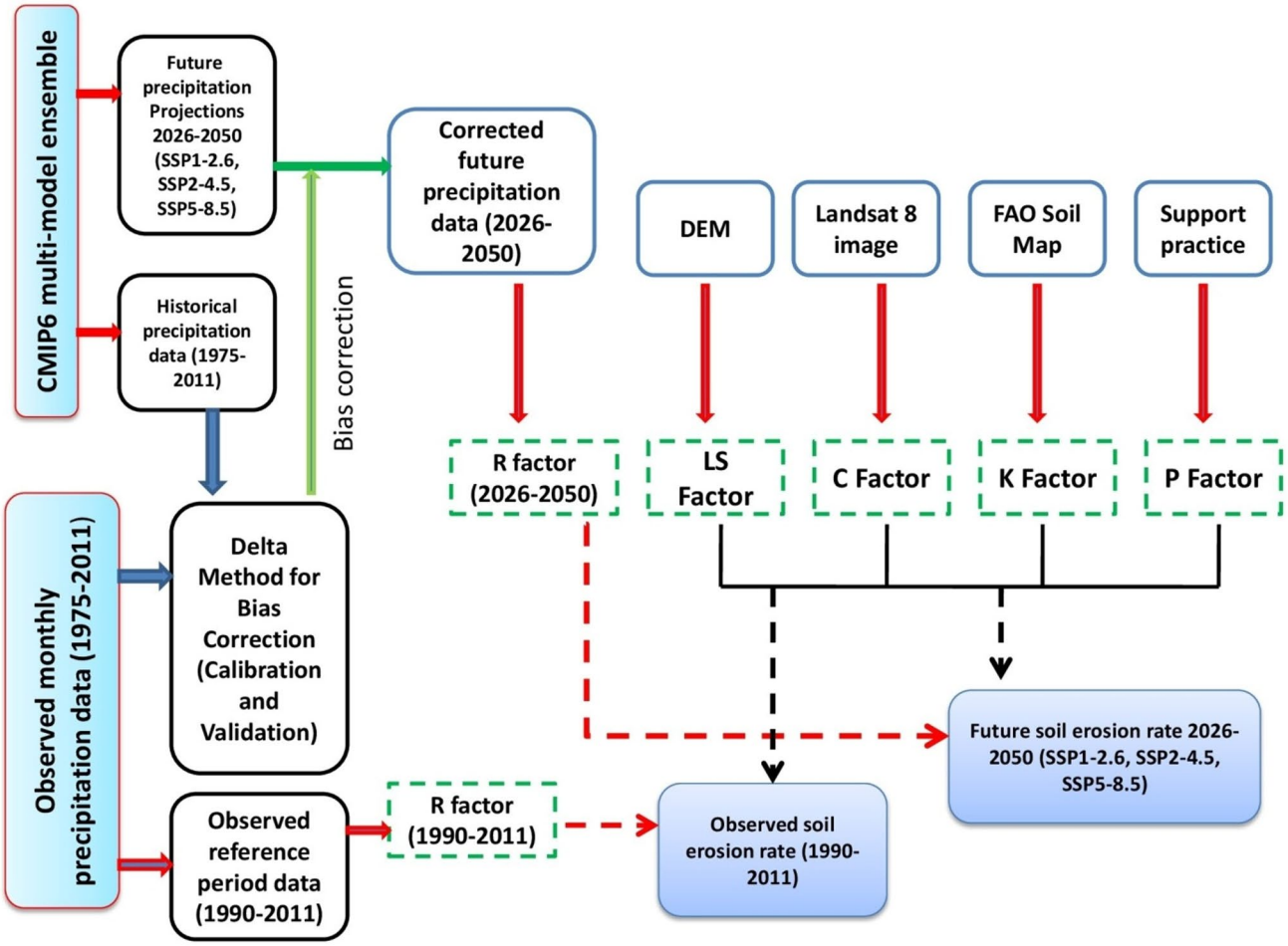

Fig. 3 Methodological framework for assessing soil erosion under observed and future climate scenarios using RUSLE

RUSLE model factors

RUSLE model (Eq. 6), is an empirical, factor-driven model that integrates rainfall, soil characteristics, topography, cropping systems, and land-management practices to estimate annual soil-erosion rates on slopes (Renard et al. 1997). Due to straightforward implementation, extensive literature, and seamless integration with GIS, USLE and its revised form, RUSLE, have become the most widely used soil erosion prediction models worldwide (Pandey et al. 2016; Alewell et al. 2019; Melalih and Mazour 2021; Sakhraou and Hasbaia 2023). However, the RUSLE model has some limitations, particularly the precise spatial evaluation of the used parameters; moreover, it does not simulate sediment transport, deposition, or gully erosion. It does not explicitly model surface runoff processes. Consequently, it is less effective in predicting erosion from individual storm events (Alewell et al. 2019).

$$\mathbf{A} = \mathbf{R} \times \mathbf{K} \times \mathbf{LS} \times \mathbf{C} \times \mathbf{P} \quad (6)$$

Here, A represents the average annual soil loss (t/ha/year), K represents the soil erosion coefficient (t.ha.h/ha.MJ.mm), LS represents the topographic coefficient (dimensionless), C represents the cover management coefficient (dimensionless), and P represents the conservation application coefficient (dimensionless).

Rainfall erosivity factor (R factor)

The erosivity factor (R) determines the ability of a rainstorm to cause soil erosion and depends largely on the intensity and kinetic energy of rainfall. The most suitable method for estimating R is the EI_{30} index (Wischmeier and Smith 1978). However, applying this method requires high-resolution data, which are not available in the study area. Therefore, we used an equation based on the modified Fourier index (Eq. 7) (Hernando and Romana 2015). This formula was tested and well recommended in the Ksob watershed adjacent to the study area (Sakhraou and Hasbaia 2023).

$$\mathrm{R} = 10.5 \times \mathrm{MFI} \quad (7)$$

$$\text{Where MFI} = \sum_{i=1}^{12} \frac{Pi^2}{P} \tag{8}$$

Here, MFI shows Modified Fourier Index, Pi is the mean monthly rainfall for month i and P is the mean annual rainfall, both in mm.

Soil erodibility factor (K factor)

The soil erodibility factor (K factor) expresses the influence of soil properties on the erodibility of a slope (Renard et al. 1997). These properties include texture, structure and organic matter content, which affect soil permeability, water-holding capacity, and infiltration rates, as well as detachment, transport, and erosion from rainfall and runoff (Alewell et al. 2019). In this study the value of K factor is calculated using the following formula (Eq. 9) proposed by Foster et al. (1981)

$$\begin{aligned} K =& 27.66 \times M^{1.14} \times 10^{-8} \times (12 - a) \\ &+ 0.0043\,(b - 2) + 0.0033(c - 3) \end{aligned} \tag{9}$$

$$M = (silt\% + sand\%) \times (100 - clay\%) \tag{10}$$

$$a = 1.72 \times OC \tag{11}$$

(Here, K is the soil erodibility factor (t h MJ1 mm1); M is the soil grain size parameter; a is the organic matter content (%); OC is the percentage of organic carbon content in the soil; b is the soil structure code: value 1 is very structured or particulate, 2 is highly structured, 3 is slightly structured, and 4 is solid; and c is the soil profile permeability code: where (1) is fast, (2) is medium to fast, (3) is medium, (4) is medium to slow, (5) is slow, and (6) is very slow.

Topographic factor (LS factor)

The LS-factor (slope length and steepness factor) accounts for how slope length and gradient influence sheet, rill, and inter-rill erosion by water. It represents the ratio of predicted soil loss from a specific slope compared to the standard USLE unit plot (Wischmeier and Smith 1978). For the calculation of topographic factor (LS), we used the formula developed by Wischmeier and Smith (1961) for the calculation of topographic factor (LS):

$$\begin{aligned} LS = & \left(Flow\ accumulation \times \frac{Resoution}{22.1} \right)^{m} \\ & \times (0.065 + 0.045 \times S + 0.0065 \times S^2) \end{aligned} \tag{12}$$

Here, S' is the slope (%) and 'm' is a parameter relative to each class of slope (Wischmeier and Smith 1978).

Crop management factor (C factor)

The C-factor (the crop and management factor) represents the influence of vegetation cover, cropping systems, land management, and erosion control practices on the rate of soil loss (Wischmeier and Smith 1978). Researchers have used several methods to estimate the C-factor, including assigning fixed values from land use/land cover classifications based on previous studies in similar environments, deriving it from high-resolution imagery through the Normalized Difference Vegetation Index (NDVI), or relying on field-based measurements when the study area is relatively small (Benavidez et al. 2018). In this study, the C factor is evaluated by Eq. (13) proposed by Van et al. (2000), based on NDVI.

$$C = e^{-\alpha \left(\frac{NDVI}{\beta - NDVI} \right)} \tag{13}$$

$$NDVI = \frac{NIB - Red}{NIB + Red} \tag{14}$$

Where: α and β are constants (α=2 and β=1, Van et al. 2000), NDVI (Normalized Difference Vegetation Index), NIB is the near infrared band, and Red is the red band.

Support practice factor (P factor)

The P-factor quantifies the reduction in soil loss provided by specific conservation practices, such as contouring, strip-cropping, or terracing, by comparing the erosion under those practices to conventional up-and-down-slope tillage (Renard et al. 1997). According to Wischmeier and Smith (1978), P-factor values generally range from around 0.2 for reverse-slope bench terraces to 1.0 in the absence of erosion-control measures, with lower values indicating more effective erosion control. Because the Wadi Al-Ham watershed lacks significant conservation structures or environmental practices, a uniform $P=1$ is applied across all plots, indicating a lack of support practices in the current land management system.

Results and discussion

Bias correction performance

Table 2; Fig. 4 summarize the statistical evaluation of bias correction performance, along with its effect on improving the simulated average annual precipitation of the historical multi-model ensemble (2000–2011) relative to observed values. It is noteworthy that the models overestimate precipitation at most stations and exhibit large variability

Table 2 Performance of the delta bias correction method

Station	PBIAS (%) before BC	PBIAS (%) after BC	RMSE (mm) before BC	RMSE (mm) after BC	nRMSE (%) before BC	nRMSE (%) after BC
S01	57.51	-8.15	31.67	24.78	169.77	132.83
S02	56.48	-0.48	31.78	23.92	158.13	119.02
S03	176.69	37.31	34.97	17.39	327.87	163.04
S04	67.82	-8.51	31.48	21.41	179.8	122.28
S05	4.00	-21.68	31.32	29.20	110.85	103.35
S06	39.32	-23.28	30.14	22.51	140.68	105.07
S07	-15.20	-31.36	25.85	25.35	151.72	148.78
S08	54.02	-23.13	32.85	27.55	184.61	154.83

compared to observed monthly precipitation, as evidenced by the high nRMSE values (greater than 100%) at all stations. This is expected in a semiarid climate with low mean monthly precipitation, meaning that even small absolute deviations can lead to large relative errors.

Bias correction significantly reduced the systematic bias (PBIAS) at most stations. For instance, S03 showed a significant decrease from +176.69% to +37.31%, while S01 and S04 shifted from strong overestimation (+57.51% and +67.82%) to slightly underestimated (-8.15% and −8.51%, respectively). RMSE also decreased at most stations by varying degrees, with the largest improvement observed at S03 (from 34.97 mm to 17.39 mm). The nRMSE values followed the same decreasing trend, but remained high (>100%) at all stations, suggesting that in this study the Delta Method had limited ability to correct variability. This limitation was particularly evident at stations S05 and S07, where S05 showed only a slight decrease in RMSE (from 31.32 mm to 29.20 mm) and a significant shift in PBIAS from +4.00% to -21.68%, while the RMSE in S07 remained almost constant (from 25.85 mm to 25.35 mm), and PBIAS deteriorated from −15.20% to -31.36%. Consequently, bias correction was not applied to these two stations, and the uncorrected model outputs were retained for the future precipitation assessment. In general, the applied bias correction method was most effective at stations with high bias before correction; while at stations with low initial bias, performance gains were limited or even negative.

Precipitation projection

In this study, the R factor was calculated using a relationship involving the Modified Fournier Index (MFI), which considers both monthly precipitation and mean annual precipitation. To provide context for the differences between climate scenarios, this section briefly presents future precipitation projections by presenting maps comparing mean annual precipitation under the three SSP scenarios with the historical reference period. Figure 5; Table 3 summarize annual precipitation maps and some relevant statistics for the reference period (1990–2011) and the future period (2026–2050) for scenarios SSP1-2.6, SSP2-4.5, and SSP5-8.5.

The results indicate the following main outcomes:

- The three future projections maintain a north-south precipitation gradient (higher precipitation values in the north and lower precipitation values in the south).
- For all three scenarios, projected mean annual precipitation is lower than in the reference period, with decreases ranging from 15 to 24% (Observation: 219.4 mm; SSP1-2.6: 184.55 mm; SSP2-4.5: 175.66 mm; SSP5-8.5: 155.15 mm).
- While there are some differences in the spatial distribution of precipitation categories among the three scenarios (although there is a constant gradient from north to south), mean total annual precipitation values remain similar.
- In the future scenarios, the low precipitation class predominates, while the medium precipitation class (at the local scale) was more prevalent in the reference period.

RUSLE factors maps

Rainfall erosivity (R)

During the historical period (1990–2011), estimated R values ranged between 312 and 460 (MJ.mm/ha.h.yr) with an average of 391 (MJ.mm/ha.h.yr) (Fig. 6), with the highest values being concentrated in the northern parts of the watershed near the Mediterranean Sea and corresponding to the highest precipitation values. As for future projections, they indicate a decrease in average values to 274 (SSP1-2.6), 271 (SSP2-4.5), and 285 (MJ.mm/ha.h.yr) (SSP5-8.5), with ranges between (207 and 445), (210 and 262), and (214 and 467), respectively. However, all scenarios maintain a clear erosivity gradient between north and south.

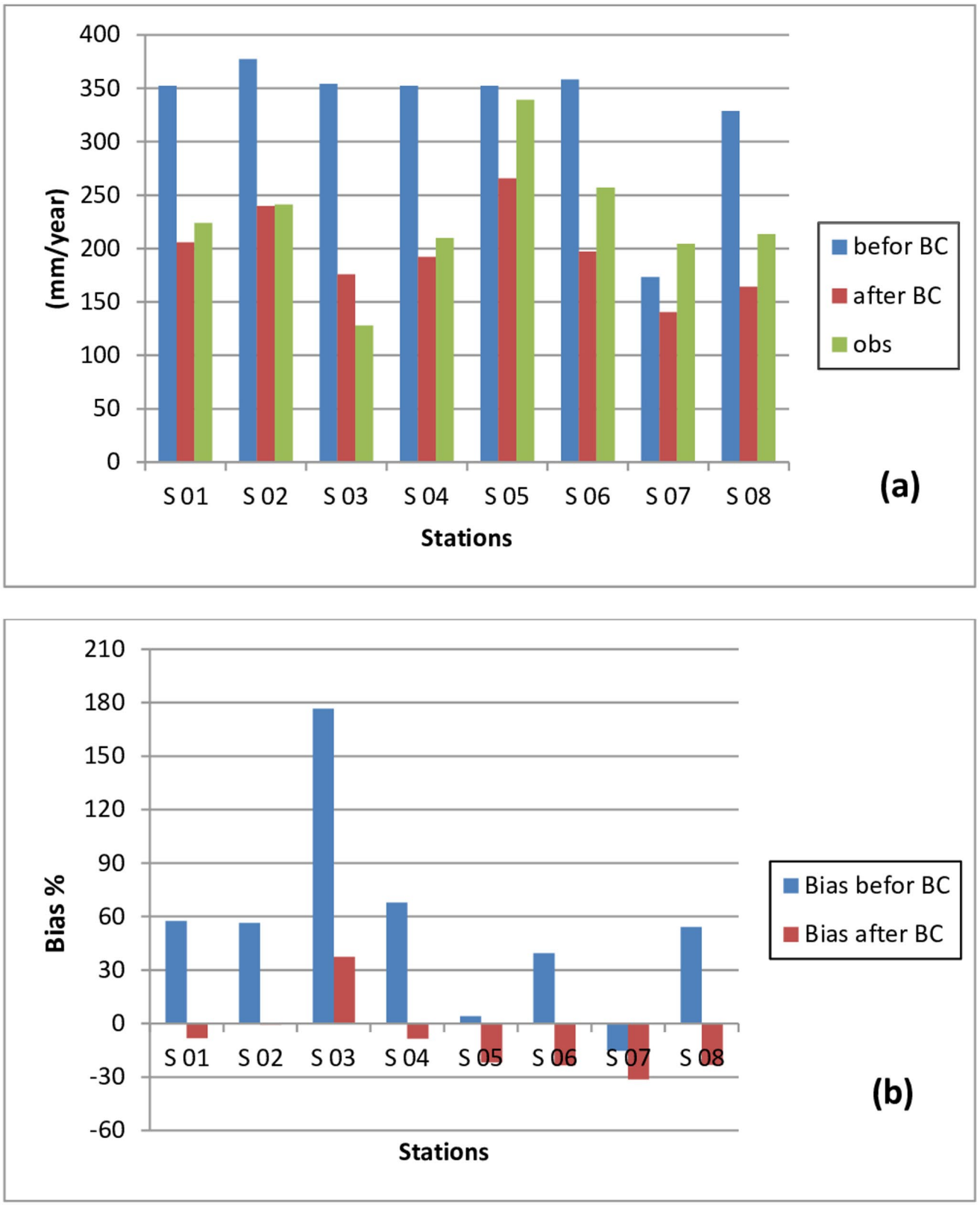

Fig. 4 (a) Average annual precipitation for the validation period (2000–2011) from historical data (from models) before and after bias correction (BC), compared to the average observed data (Obs). (b) Bias (%) between historical and observed data before and after bias correction

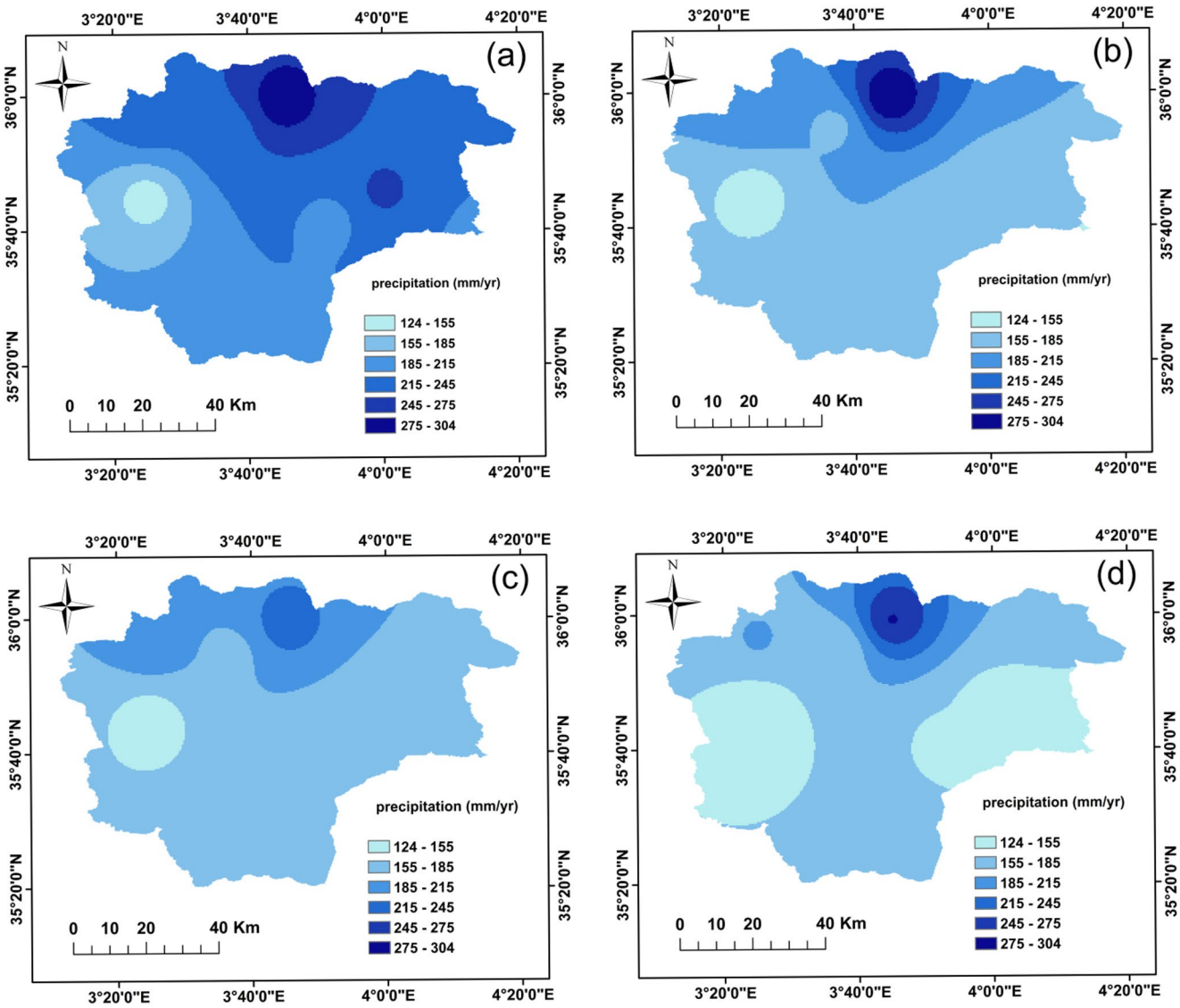

Fig. 5 Annual precipitation maps: (a) observed reference period (1990–2011), (b) SSP1-2.6, (c) SSP2-4.5, and (d) SSP5-8.5 for the future period (2026–2050)

Table 3 Summary statistics of observed and projected annual precipitation for the reference (1990–2011) and future period (2026–2050)

Period / Scenario	124–155 mm/yr (%)	155–185 mm/yr (%)	185–215 mm/yr (%)	215–245 mm/yr (%)	245–275 mm/yr (%)	275–304 mm/yr (%)	Mean Annual precipitation (mm/yr)	min (mm/yr)	max (mm/yr)
Observed 1990–2011	1.66	8.63	35.18	42.41	9.13	2.96	219.4	142	295.23
SSP1–2.6 (2026–2050)	4.24	63.7	22.32	4.29	3.29	2.13	184.55	137.87	303.43
SSP2–4.5 (2026–2050)	5.13	74.06	17.59	3.2	0	0	175.66	138	232.27
SSP5–8.5 (2026–2050)	31.75	42.45	16.53	6.56	2.61	0.076	166.15	124.36	276.23

Topographic factor (LS)

This factor ranges from 0 to 6.51 with an average of 0.22 as in Figure 7a, with the highest values recorded on the steep northern slopes. Although these cells with high LS cover a small portion of the watershed, they correspond to areas with a high risk of erosion, confirming the role of slope steepness and length in increasing soil loss.

C values across the watershed range from 0.107 to 1.37, with an average value of approximately 0.79 (see Fig. 7b), This reflects differences in vegetation and land use. The highest C values, indicating decreasing land cover and increasing erosion susceptibility, are recorded in most of the

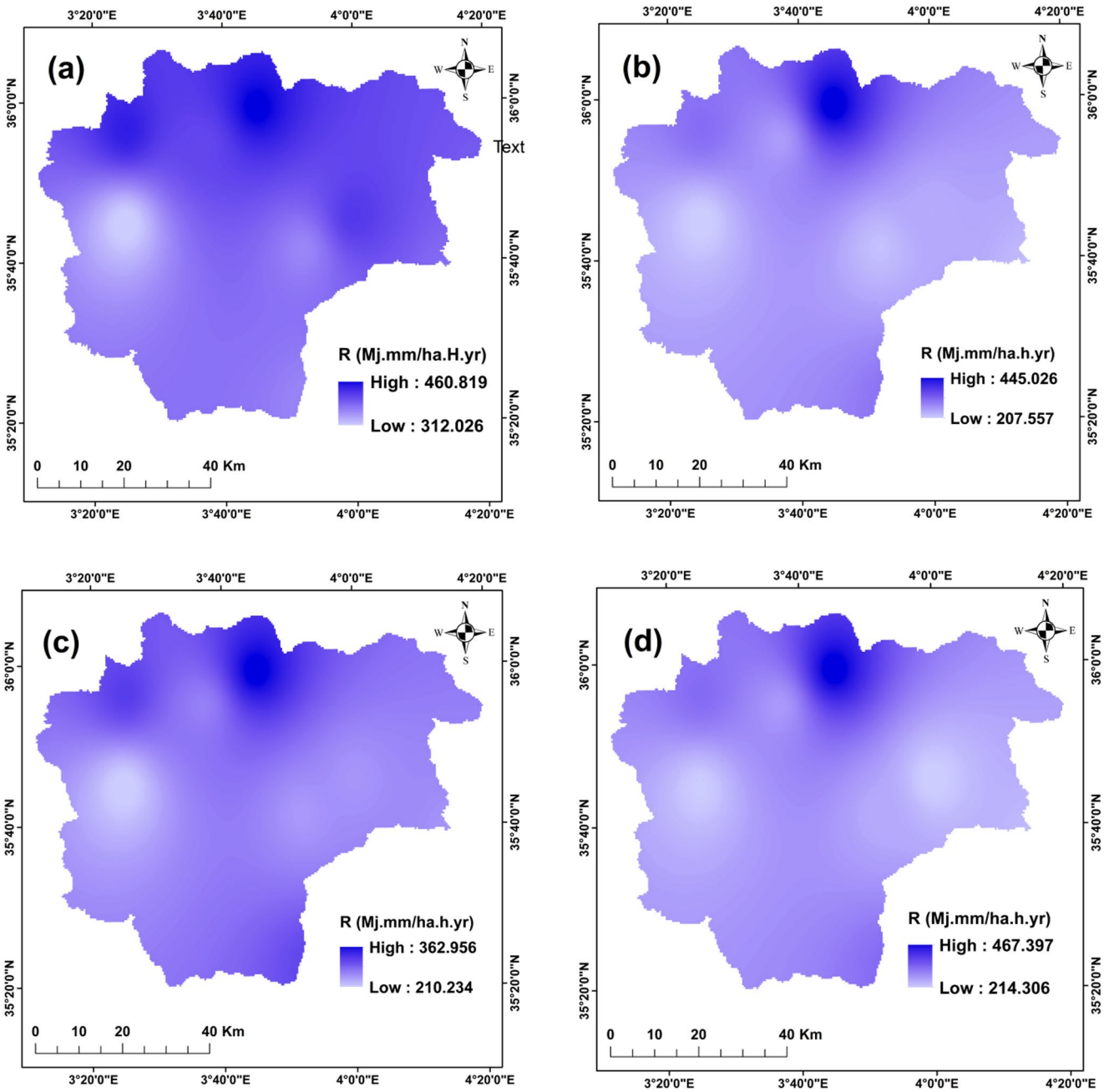

Fig. 6 Spatial distribution of the rainfall erosivity factor (R): (a) observed reference period (1990–2011), (b) SSP1-2.6, (c) SSP2-4.5, and (d) SSP5-8.5 for the future period (2026–2050)

northern half of the watershed, where vegetation cover is exceptionally low. However, an exception can be seen in a narrow northern strip dominated by dense forests, which corresponds to the lowest C values (close to 0.107). In the rest of the region, the central and southern parts show low to moderate vegetation density, offset by moderate C values, confirming their partial protective effect against erosion.

Soil erodibility (K)

In Figure 7c, K values in the watershed range from 0.0373 to 0.0818 (t ha h/ha MJ mm), with an average of 0.0631 (t ha h/ha MJ mm), reflecting moderate erosion susceptibility in various dominant soil types. Table 4 provides more details on the K factor calculation.

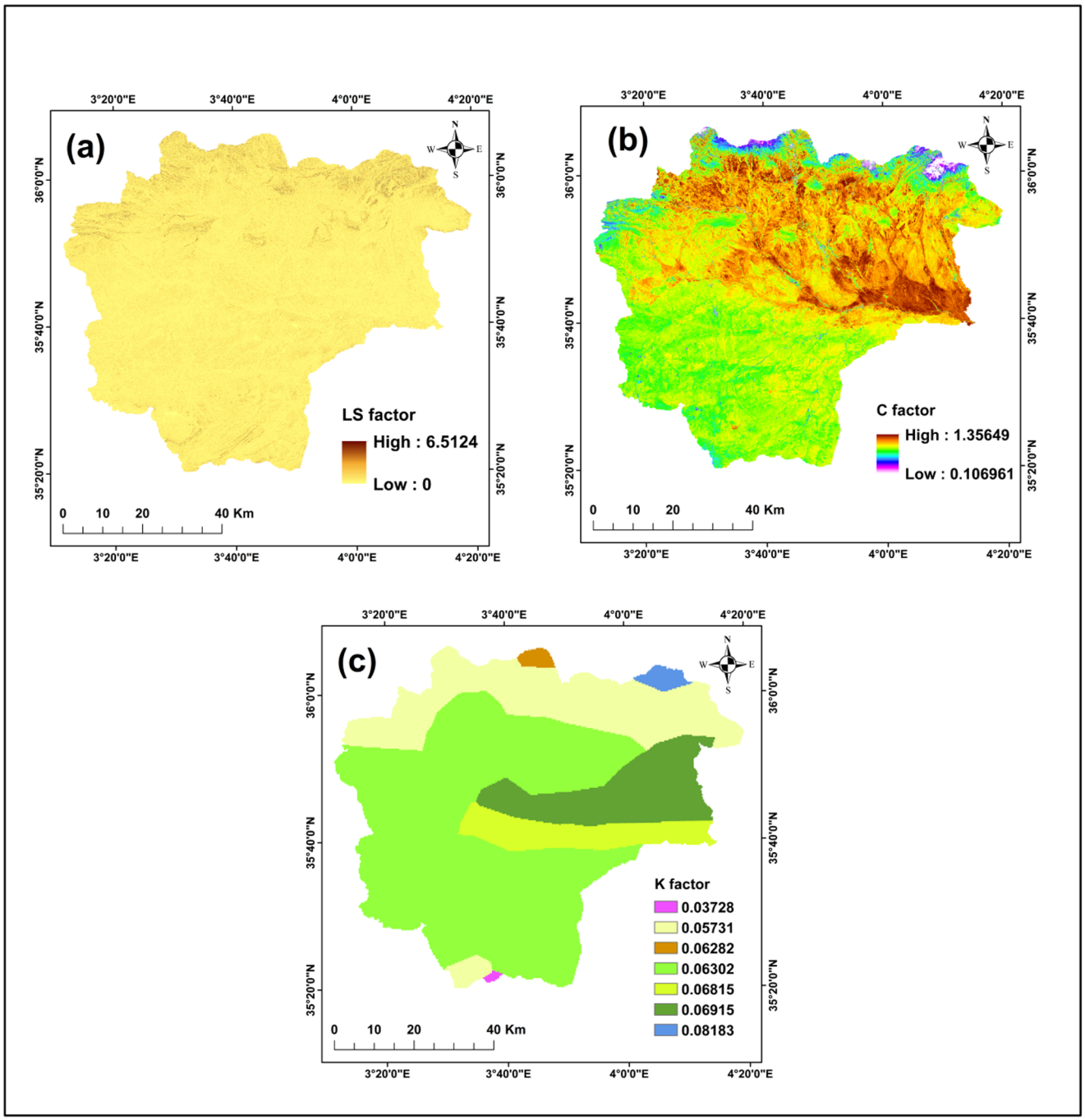

Fig. 7 (a) Topographic Factor (LS) (b) Cover management factor map (C factor) (c) Soil Erodibility Factor (K)

Table 4 Details of K factor calculation

Soil sample	MS (sand) top soil %	msilt (silt) top soil %	MC (clay) topsoil %	orgC oraganic carbon %	M	a	b	c	K factor
BC	81.6	6.8	11.7	0.44	7805.72	0.7568	2	2	**0.08183**
XK	48.7	29.9	21.6	0.64	6162.24	1.1008	2	3	**0.06303**
I	58.9	16.2	24.9	0.97	5640.01	1.6684	2	4	**0.05731**
LC	64.3	12.2	23.5	0.63	5852.25	1.0836	2	4	**0.06282**
YK	63.5	17.9	18.7	0.26	6617.82	0.4472	2	2	**0.06917**
ZG	47.8	8.5	43.8	0.38	3164.06	0.6536	2	5	**0.03729**
YH	50.4	29	20.6	0.3	6304.36	0.516	2	3	**0.06816**

Bold values indicate calculated K-factor values

Historical and projected specific erosion Estimation

Figure 8; Table 5 show the maps and rates of soil erosion in the Wadi Al-ham watershed for the historical and future periods under the three climate scenarios.

Historical erosion

During the historical period (1990–2011), estimated soil loss in the watershed ranged from 0 to 86 t ha^{-1} yr^{-1}, with an overall average of 5.18 t ha^{-1} yr^{-1}. When divided into four erosion-risk classes, low erosion (0–2 t ha^{-1} yr^{-1}) occupied 56% of the area, moderate erosion (2–5 t ha^{-1} yr^{-1}) about 11%, high erosion (5–10 t ha^{-1} yr^{-1}) 18%, and very high erosion (> 10 t ha^{-1} yr^{-1}) 15%. The steep, high-rainfall

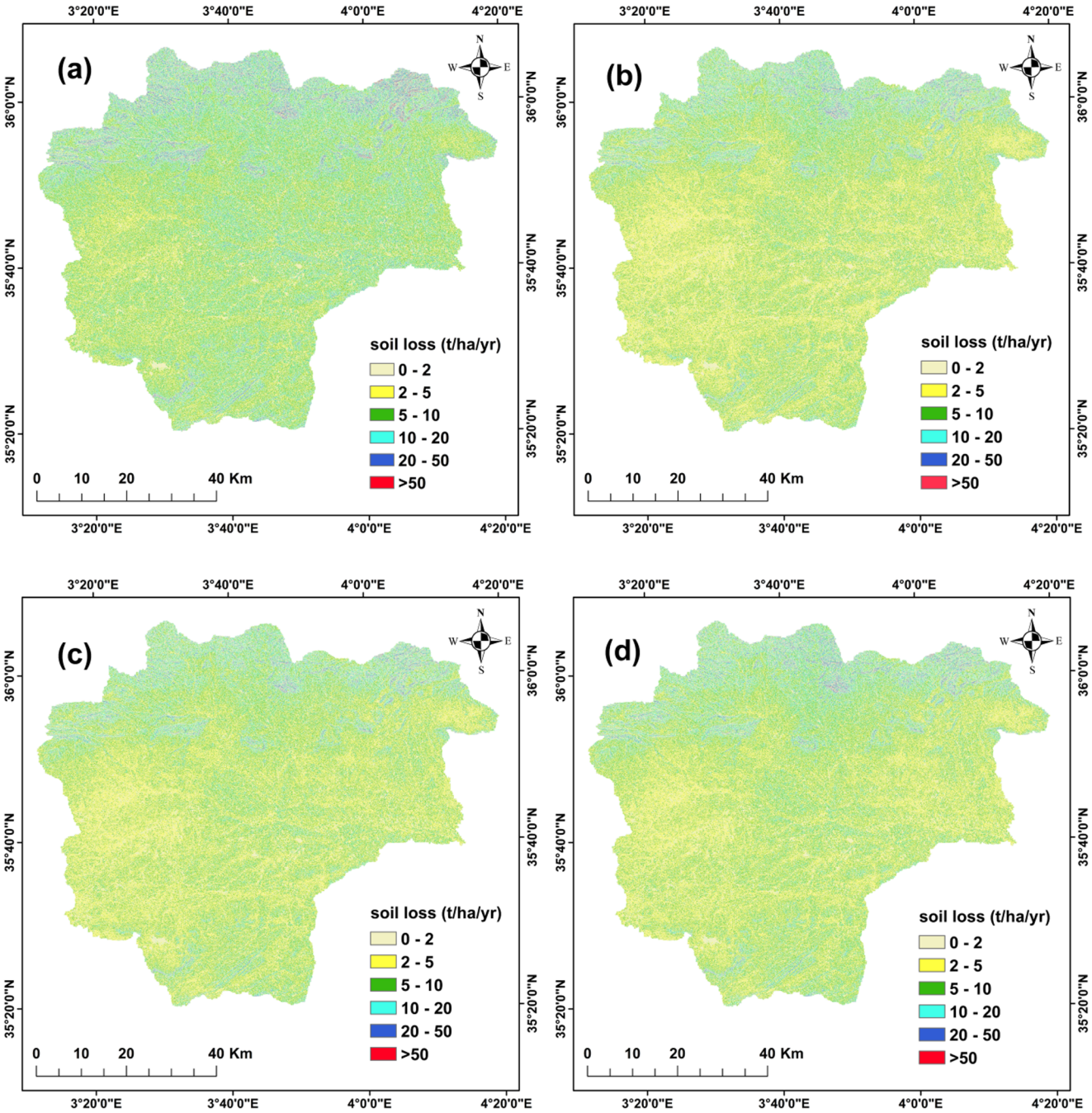

Fig. 8 Annual soil erosion (t ha^{-1} yr^{-1}): (a) observed reference period (1990–2011), (b) SSP1-2.6, (c) SSP2-4.5, and (d) SSP5-8.5 for the future period (2026–2050)

Table 5 Mean annual soil erosion (t ha^{-1} yr^{-1}) and class distribution (%) for the observed period and future scenarios

Period/Scenario	0–2 t/ha/yr (%)	2–5 t/ha/yr (%)	5–10 t/ha/yr (%)	10–20 t/ha/yr (%)	20–50 t/ha/yr (%)	>50 t/ha/yr (%)	Mean Annual Soil Loss (t/ha/yr)
Observed 1990–2011	56.09	10.4	18.32	12.21	2.89	0.058	5.18
SSP1–2.6 (2026–2050)	58.42	17.55	16.56	6.4	1.03	<0.01	3.77
SSP2–4.5 (2026–2050)	58.35	17.5	16.93	6.34	0.86	<0.01	3.72
SSP5–8.5 (2026–2050)	58.07	16.79	16.95	6.97	1.18	0.0106	3.91

northern sectors of the watershed exhibit the highest erosion rates, whereas central and southern zones, characterized by gentler slopes, fall predominantly within the low-erosion classes. This result is consistent with observed measurements obtained using a hydrometric station and suspended sediment sampling at the outlet of the watershed, as reported by Hasbaia et al. (2012) for the same watershed (5.3 t/ha/year for 1968–1989), and with Djoukbala et al. (2022), who estimated 6.1 t/ha/year for the large Hodna basin that includes the Wadi Al-Ham watershed, which judge the good quality of the obtained results.

Future erosion

Under the future climate scenarios used over the period (2026–2050), the obtained specific erosion does not show any significant difference among the results; mean annual erosion decreases to 3.77 t ha^{-1} yr^{-1} for SSP1-2.6 (SD = 4.61), 3.72 t ha^{-1} yr^{-1} for SSP2-4.5 (SD = 4.47), and 3.91 t ha^{-1} yr^{-1} for SSP5-8.5 (SD = 4.80). The low-erosion class increases to about 58% of the watershed, while both moderate and high-erosion categories expand slightly to roughly 16–17%. Very high erosion contracts to approximately 7–8% of the area. Spatially, vulnerability remains greatest in the northern highlands and select southern slopes, with central and southern portions continuing to experience predominantly low to moderate soil loss.

Discussion of uncertainties

While our results indicate that average soil erosion rates will decrease under future climate change scenarios, it is not possible to confirm that these rates will decrease due to numerous sources of uncertainty that cannot be ignored. In this context, de Vente and Eekhout (2020) conducted a study on the effect of differences in soil erosion models, bias correction methods, and the size of the ensemble of climate models used for the results of soil erosion assessment in the context of climate change, especially in two water basins in southeastern Spain, where a decrease in annual precipitation is expected with an increase in extreme precipitation events due to climate change. They tested the following points.

(1) Three soil erosion models: RUSLE (forced by precipitation), MUSLE (forced by runoff) and SPHY-MMF (forced by precipitation and runoff).

(2) Three methods for bias correction: Delta change (DC), Quantile mapping (QM), and scaled distribution mapping (SDM).

(3) For climate models, evaluate the use of single models versus the use of a multi-model ensemble.

The results for soil models and bias correction methods ranged between a decrease in expected soil erosion (RUSLE, DC), an increase (MUSLE, QM), and a mixed result between them (MMF, SDM). Regarding climate models, the results showed that the use of individual models may show an opposite trend to the multi-model ensemble average. Finally, they concluded as a result that it is better to use a model of erosion forced by precipitation and runoff together, in the case of a conflict between total precipitation and extreme precipitation events resulting from climate change. The bias correction method has the best performance in reproducing the expected climate change signal. To evaluate the effects of climate change on soil erosion, there is a need to use a multi-model ensemble average containing enough climate models.

Our results, interpreted based on the results of de Vente and Eekhout (2020), indicate an expectation of a decrease in soil erosion in the future, based on our use of the (RUSLE) model, which does not capture the effects of changes in the intensity and frequency of extreme precipitation events and the resulting runoff, and the delta bias correction method, which underestimates the expected mean precipitation. This reduction in expected erosion is due to uncertainty arising from the concept of the soil erosion model and the bias-correction method, which fails to capture the projected climate change signal. However, the selection of a particular approach or model for erosion prediction is heavily dictated by the required data, which are not always available in terms of time accuracy or the density of monitoring stations, particularly in developing countries, which are particularly affected by this problem. This requires researchers to use models that do not require high-resolution data or rely on satellite data, introducing uncertainty that cannot be ignored.

Conclusion

In this study, the RUSLE model was applied to evaluate historical (1990–2011) and future (2026–2050) soil erosion in Wadi Al-Ham watershed using bias-corrected monthly precipitation data of Cimp6 multi-model ensemble under SSP1-2.6, SSP2-4.5 and SSP5-8.5.

The bias-correction performance of the Delta method showed that it significantly reduced systematic bias (PBIAS) in most cases; however, its ability to correct for variability in this study was limited. The results show that historical specific erosion in the Wadi El-Ham watershed was 5.18 tons/ha/year, with the highest soil losses recorded on the steep northern slopes and low erosion rates in more than half of the watershed. Future projections (2026–2050) indicate a 24–28% reduction in average soil loss across the scenarios. Additionally, areas with extremely high erosion have decreased to 7–8% compared to the historically observed 15%. However, northern regions remain the most vulnerable to erosion, requiring targeted measures to protect soils.

However, it is important to note a key factor affecting the accuracy of the results: biases in climate model outputs, the bias correction method used, and the concept of the soil erosion model applied. Climate models may overestimate (or underestimate) precipitation, while bias correction methods do not perform equally well. In addition, empirical models such as RUSLE suffer from several limitations; For example, they do not account for sediment transport or the dynamics of vegetation cover. Further research combining climate change and land-use scenarios, testing multiple bias correction methods and runoff-based erosion models, and conducting field validation would improve soil erosion estimates.

Author contributions The authors K.D. and M.H. contributed to the design and conception of the study. K.D. and O.D. collected and analyzed the data. Z.S. reviewed the manuscript and corrected its language. All authors reviewed and approved the final manuscript.

Data availability No datasets were generated or analysed during the current study.

Declarations

Conflict of interest The authors declare no competing interests.

References

Alewell C, Borrelli P, Meusburger K, Panagos P (2019) Using the USLE: chances, challenges and limitations of soil erosion modelling. Int Soil Water Conserv Res 7(3):203–225

Almazroui M, Saeed F, Saeed S, Nazrul Islam M, Ismail M, Klutse NAB, Siddiqui MH (2020) Projected change in temperature and precipitation over Africa from CMIP6. Earth Syst Environ 4:455–475

Bammou Y, Benzougagh B, Bensaid A, Igmoullan B, Al-Quraishi AMF (2024) Mapping of current and future soil erosion risk in a semi-arid context (haouz plain-Marrakech) based on CMIP6 climate models, the analytical hierarchy process (AHP) and RUSLE. Model Earth Syst Environ 10(1):1501–1514

Belazreg NEH, Hasbaia M, Şen Z, Ferhati A (2023) Historical evaluation and future projections of monthly precipitation and temperature under CMIP6 gcms, case of hodna basin (central Algeria). Arab J Geosci 16(1):39

Benavidez R, Jackson B, Maxwell D, Norton K (2018) A review of the (Revised) universal soil loss equation ((R) USLE): with a view to increasing its global applicability and improving soil loss estimates. Hydrol Earth Syst Sci 22(11):6059–6086

Beyer R, Krapp M, Manica A (2020) An empirical evaluation of bias correction methods for palaeoclimate simulations. Clim Past 16(4):1493–1508

Borrelli P, Robinson DA, Fleischer LR, Lugato E, Ballabio C, Alewell C, Meusburger K, Modugno S, Schütt B, Ferro V, Bagarello V (2017) An assessment of the global impact of 21st century land use change on soil erosion. *Nature communications*, *8*(1), p.2013

Borrelli P, Alewell C, Alvarez P, Anache JAA, Baartman J, Ballabio C, Bezak N, Biddoccu M, Cerdà A, Chalise D, Chen S (2021) Soil erosion modelling: A global review and statistical analysis. Sci Total Environ 780:146494

Chetioui C, Bouregaa T (2024) Temperature and precipitation projections from CMIP6 for the Setif high plains in Northeast Algeria. Arab J Geosci 17(2):63

de Vente J, Eekhout J (2020) The implications of soil erosion model conceptualization, bias-correction methods and climate model ensembles on soil erosion projections under climate change, EGU General Assembly Online, 4–8 May 2020, EGU2020-8158. https://doi.org/10.5194/egusphere-egu2020-8158, 2020

Djoukbala O, Hasbaia M, Benselama O, Hamouda B, Djerbouai S, Ferhati A (2022) Water erosion and sediment transport in an ungauged semiarid area: the case of Hodna Basin in Algeria. *Wadi Flash Floods: Challenges and Advanced Approaches for Disaster Risk Reduction*, pp.439–454

Foster GR, McCool DK, Renard KG, Moldenhauer WC (1981) Conversion of the universal soil loss equation to SI metric units. J Soil Water Conserv 36(6):355–359

García-Ruiz JM, Beguería S, Lana-Renault N, Nadal-Romero E, Cerdà A (2017) Ongoing and emerging questions in water erosion studies. Land Degrad Dev 28(1):5–21

Hamitouche Y, Zeroual A, Meddi M, Assani AA, Alkama R, Şen Z, Zhang X (2024) Projected Changes in Extreme Precipitation Patterns across Algerian Sub-Regions. Water 16(10):1353

Hasbaia M, Hedjazi A, Benayada L (2012) Variabilite de l ' érosion hydrique Dans Le Bassin du hodna: Cas du Sous-Bassin versant de l ' Oued Elham. Revue Marocaine Des Sci Agronomiques Et Vétérinaires 1(1):28–32

Hernando D, Romana MG (2015) Estimating the rainfall erosivity factor from monthly precipitation data in the Madrid Region (Spain). J Hydrol Hydromech 63(1):55

Hughes DA, Mantel S, Mohobane T (2014) An assessment of the skill of downscaled GCM outputs in simulating historical patterns of rainfall variability in South Africa. Hydrol Res 45(1):134–147

Jarray F, Hermassi T, Sellami H, Ben Abdallah MA, Mechergui M (2025) Assessing Spatial soil erosion under climate change using SWAT model in a Semi-Arid watershed of Northeastern Tunisia. Environmental Research Communications

Lamane H, Mouhir L, Zouahri A, Baghdad B, Bilali E, A. and, Moussadek R (2025) Modeling soil erosion and sediment yield under climate change: a comparison of RUSLE and MUSLE integrated

with SDR using variable soil data resolutions. Model Earth Syst Environ 11(5):1–29
Li Z, Fang H (2016) Impacts of climate change on water erosion: A review. Earth Sci Rev 163:94–117
Melalih A, Mazour M (2021) Using RUSLE and GIS for the soil loss assessment in arid regions: the case of the Ain Sefra catchment in the Ksour Mountains, Algeria. J Water Land Dev (48)
Mendez M, Maathuis B, Hein-Griggs D, Alvarado-Gamboa LF (2020) Performance evaluation of bias correction methods for climate change monthly precipitation projections over Costa Rica. Water 12(2):482
Pandey A, Himanshu SK, Mishra SK, Singh VP (2016) Physically based soil erosion and sediment yield models revisited. CATENA 147:595–620
Pandey S, Kumar P, Zlatic M, Nautiyal R, Panwar VP (2021) Recent advances in assessment of soil erosion vulnerability in a watershed. Int Soil Water Conserv Res 9(3):305–318
Raza A, Ahrends H, Habib-Ur-Rahman M, Gaiser T (2021) Modeling approaches to assess soil erosion by water at the field scale with special emphasis on heterogeneity of soils and crops. Land 10(4):422
Remini B, Hallouche W (2007) Studying sediment. Revue International Water Power et Dam construction. Octobre, pp.42–45
Renard K, Foster G, Weesies G et al (1997) Predicting soil erosion by water: a guide to conservation planning with the revised universal soil loss equation (RUSLE). Agric Handb 703
Sahabi-Abed S, Ayugi BO, Selmane ANEI (2023) Spatiotemporal projections of extreme precipitation over Algeria based on CMIP6 global climate models. Model Earth Syst Environ 9(3):3011–3028
Sakhraoui F, Hasbaia M (2023) Evaluation of the sensitivity of the RUSLE erosion model to rainfall erosivity: A case study of the Ksob watershed in central Algeria. Water Supply 23(8):3262–3284
Sartori M, Philippidis G, Ferrari E, Borrelli P, Lugato E, Montanarella L, Panagos P (2019) A linkage between the biophysical and the economic: assessing the global market impacts of soil erosion. Land Use Policy 86:299–312
Sauchyn Dave J, Belanger MR, Anis S, Basu, Sheena Stewart (2022) Understanding and accommodating uncertainty in climate change data. A Climate West Primer
Schmidli J, Frei C, Vidale PL (2006) Downscaling from GCM precipitation: a benchmark for dynamical and statistical downscaling methods. Int J Climatology: J Royal Meteorological Soc 26(5):679–689
Van der Knijff JM, Jones RJA, Montanarella L (2000) *Soil erosion risk assessment in Europe* [online]
Weng X, Zhang B, Zhu J, Wang D, Qiu J (2023) Assessing land use and climate change impacts on soil erosion caused by water in China. Sustainability 15(10):7865
Wischmeier W, Smith D (1961) A universal equation for predicting rainfallerosion losses—an aid to conservation farming in humid regions. US Dept Agric, Agr Res Serv ARS Spec Rep 22–66
Wischmeier WH, Smith DD (1978) Predicting rainfall erosion losses-a guide to conservation planning. Predict rainfall Eros losses-a Guid to Conserv planning